Chapter 2

Stochastic Theory

In classical mechanics the two-body problem always has the exact analytical solution in quadratures (e.g., see [10]). One naturally arises a question about existence of an analogous solution for the three-body problem. The final answer on this question was found in a recent time only, and, we emphasize, it was found namely due to using of the computer modeling. It turns out to be that, excepting exotic cases (which, however, play the extremely important role in physics, see below Chapter 6), the exact solution does not exist, and the system motion is stochastic. The history of developing of the stochastic theory is a classical example how, extremely simplifying the models and then studying them with the help of a computer, it becomes possible to solve the problem. In the present Chapter we describe these stochastic models, concentrating attention on the methods of their computer investigation. For a more detailed acquaintance with the stochastic theory we may recommend to refer to the monographs of Arnold and Avez [11], Sinai [12], Chirikov [13], Lichtenberg and Liberman [14], Rabinovich and Trubetskov [15], Zaslavsky [16], Schuster [17], and Arnold [18].

2.1 Hénon-Heiles model

Three-dimensional motion of a system consisting of three point particles interacting via central forces is the problem with nine degrees of freedom. However, because we always can associate a plane with three points, the problem reduces to one with six degrees of freedom. Also we can exclude two degrees of freedom, if we will use the coordinate system coupled with the center of mass of the system. However, a more radical simplification can be obtained, if we artificially "pin" two particles, and allow to move to the third particle only (see Fig. 2.1). Such a procedure may be physically justified, if we assume that one of three particles is essentially lighter, than the two other particles, for example, that it corresponds to a planet moving in the field of a double star. In such a way we come to the so-called *restricted three-body problem*, i.e., to the problem of the two-dimensional motion of a particle subjected to an external potential $V(x, y)$.

To proceed further, we have to take the concrete form for the function $V(x, y)$. Let us expand the potential $V(x, y)$ in Taylor series in vicinity of one of its minima, and take the coordinates of this minimum as the beginning of coordinates. The expansion must include the cubic terms as the minimal approximation, because the square expansion leads to the problem of two harmonic oscillators which has the trivial solution. Thus, the expansion has the form

$$\begin{aligned} V(x,y) &= V_0 + V'_x x + V'_y y + \frac{1}{2}V''_{xx}x^2 + \frac{1}{2}V''_{yy}y^2 + V''_{xy}xy \\ &+\frac{1}{6}V'''_{xxx}x^3 + \frac{1}{2}V'''_{xxy}x^2 y + \frac{1}{2}V'''_{xyy}xy^2 + \frac{1}{6}V'''_{yyy}y^3 + \cdots \end{aligned} \tag{2.1}$$

Let us take the origin of the energy scale so that $V_0 = 0$. Because the expansion of $V(x, y)$ has been done at the minimum, we have $V'_x = V'_y = 0$. Choosing appropriate directions for the x and y axes, we always can make $V''_{xy} = 0$ for the crossing term in Eq. (2.1) (such coordinates are known as the *normal coordinates*). Last, let us suppose that the "pinned" particles are identical each other, so that the potential $V(x, y)$ is even

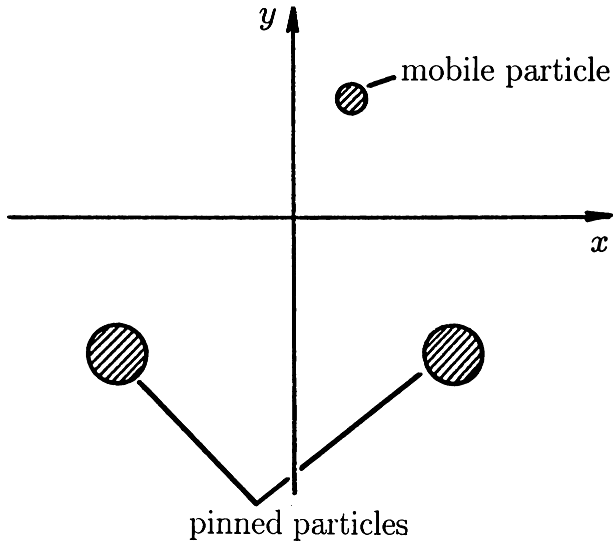

Figure 2.1: The restricted three-body problem.

in x (see Fig. 2.1), that gives $V'''_{xxx} = 0$ and $V'''_{xyy} = 0$. In the result we obtain the most simple Hamiltonian which saves all main features of the original three-body problem.

The next step is to introduce the dimensionless units. It is natural to take the mass of the mobile particle as the unit of mass. It is convenient also to choose the time unit in a way that the frequency of normal vibrations along the x axis is equal 1, and the unit of length in such a way that the coefficient at the x^2y term (which is the main term in the given problem) being equal 1 too. Finally we get the Hamiltonian (the dot denotes the derivative with respect to time)

$$H(x, \dot{x}, y, \dot{y}) = \frac{1}{2}(\dot{x}^2 + \dot{y}^2 + x^2 + \omega_y^2 y^2) + x^2 y + \mu y^3, \tag{2.2}$$

which depends on two parameters $\omega_y^2 = V''_{yy}(0,0)$ and $\mu = \frac{1}{6}V'''_{yyy}(0,0)$ only. For numerical investigation of the model we have to take numerical values for these parameters, and then to test how the results will be changed with variation of these parameters. Hénon and Heiles [19] who first proposed and investigated the model (2.2), have put $\omega_y = 1$ and $\mu = -\frac{1}{3}$.

Using Hamiltonian (2.2), we can write the motion equations:

$$\left\{ \begin{array}{rcl} \ddot{x} & = & -\partial V/\partial x\,, \\ \ddot{y} & = & -\partial V/\partial y\,. \end{array} \right. \tag{2.3}$$

Instead of the system of two differential second-order equations (2.3), usually it is more convenient to solve the system of four differential first-order equations

$$\left\{ \begin{array}{rcl} \dot{x} & = & v_x\,, \\ \dot{v}_x & = & -\partial V/\partial x\,, \\ \dot{y} & = & v_y\,, \\ \dot{v}_y & = & -\partial V/\partial y\,. \end{array} \right. \tag{2.4}$$

Then, choosing some initial conditions, we have to solve these equations for a time $t_{\max}$. However, it is too problematic to find directly from the shape of the trajectory of the system motion, wether the given problem has the solution in an integral form, or has not. Therefore, to finish the setting of the model, we have also to invent a method how we can find the answer on this question from the trajectory of the system motion.

In classical mechanics there exists the theorem which states: In order for a Hamiltonian system with N degrees of freedom to have an analytical solution, it must have N integrals of motion (the proof of

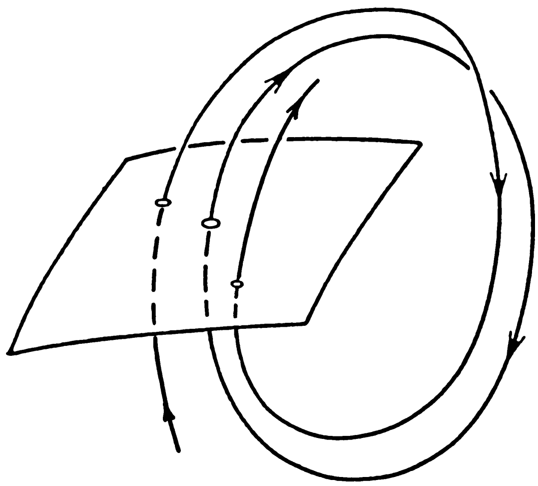

Figure 2.2: Construction of the Poincaré map.

this theorem may be found, e.g., in [11]). For example, if $V(x,y) = V^{(x)}(x) + V^{(y)}(y)$, the problem has two integrals of motion (the energies of motion along the x and y axes correspondingly), and it has the analytical solution, because the problem is split into two independent problems connected with the separated one-dimensional motions along the x and y axes. For Hamiltonian system we always have one integral of motion, that is the total energy of the system,

$$H(x, \dot{x}, y, \dot{y}) = E = \mathrm{Const}_E. \tag{2.5}$$

Thus, in order for the system (2.4) to have the analytical solution, it must exist a function $J(x, \dot{x}, y, \dot{y})$ (and $J \not\equiv H$) such that

$$J(x, \dot{x}, y, \dot{y}) = \mathrm{Const}_J \tag{2.6}$$

provided $x(t)$, $\dot{x}(t)$, $y(t)$, and $\dot{y}(t)$ are solutions of the system (2.4).

Evolution of the system with two degrees of freedom may be described as a motion of a point in the four-dimensional phase space. Due to existence of the energy conservation law, this point must move on some three-dimensional hypersurface defined by Eq. (2.5). Let us assume now that it exists the second integral of motion J. Then, Eq. (2.6) will define the second three-dimensional hypersurface, and the point associated with the system coordinates in the four-dimensional phase space, must be confined to both hypersurfaces (2.5) and (2.6) simultaneously, i.e., the point must move on the two-dimensional surface which is the intersection of two hypersurfaces (2.5) and (2.6). Then, let us take a plane (called the *section plane*) which is intersecting with this two-dimensional surface (for example, Hénon and Heiles [19] used the $Y0\dot{Y}$ plane). The intersection will occur along a curve. It is easily to see that the points of intersection of the trajectory of the system motion in the phase space with the section plane must be confined to this curve.

Thus, the problem of computer modeling reduces to the computation of coordinates of the points where the trajectory of system motion intersects with the section plane, and the latter may be chosen more or less arbitrary (see Fig. 2.2). The construction described above is known as the *Poincaré map.* If this map consists of isolated points, or if all the intersection points form a curve, the problem, may be, has the second integral of motion and, therefore, it could have an analytical solution (which, however, still has to be found). But if we can not associate a curve with the intersection points, then, most probably, the analytical solution does not exist. Notice that usually the Poincaré map has to be calculated with $\geq 10^3$ points.

The obtained by Hénon and Heiles [19] results of computer modeling are shown in Fig. 2.3. As seen, as far as the system energy E is lower than some "critical" value E_{crit} ($E_{\mathrm{crit}} = 0.115$ for the given choice of the parameters), one can plot the curves described above (different curves in Fig. 2.3a correspond to different

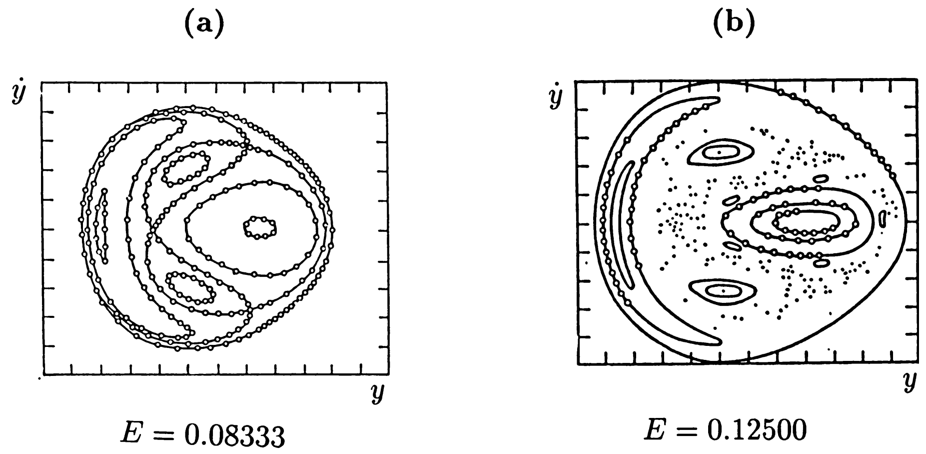

Figure 2.3: Poincaré map for the Hénon-Heiles model (2.2) at (a) $E = 0.08333$ and (b) $E = 0.12500$ (after [19]).

initial conditions). However, when $E > E_{\text{crit}}$, for some initial conditions we can plot a curve (this is the so called *islands of stability*), but for other initial conditions the sequence of points of the Poincaré map covers some region (the so-called *stochastic region*), and it is impossible to associate a smooth curve which connects these points (see Fig. 2.3b). Moreover, when we take as the initial condition different points outside the islands of stability, we always obtain the picture which seems to be practically the same. According to the established terminology, the motion within the islands of stability is called the *regular motion*, while the motion outside the islands is named by the *stochastic motion*. Below we will show that the stochastic motion really corresponds to "true chaos".

Thus, the computer modeling of the Hénon-Heiles model showed that at $E < E_{\text{crit}}$ the motion seems to be regular and an analytical solution seems to exist, while at $E > E_{\text{crit}}$ the second constant of motion is "destroyed", the stochastic region appears, and the area of the stochastic region increases (while the total area of the islands of stability decreases) with increasing of E (notice that in fact the behavior of Hamiltonian systems is more complicated, see below Sec. 2.6). However, it remains unclear *why* and *how* does the stochastic motion emerge, and *what does it look like.* To make clear these questions, the model with two degrees of freedom occurs to be too complicated, and we have to invent a more simple model which at the same time should save the main features of the phenomenon under investigation. On the other hand, the system with one degree of freedom exhibits no chaos, because it always can be exactly integrated. Thus, we have to invent the model with $1\frac{1}{2}$ degrees of freedom, i.e. a system which evolutes according to three first-order differential equations. Such a system, however, will be not a conservative system but the dissipative one.

2.2 Driven pendulum

In the previous Section we have considered in fact the system of two nonlinearly coupled oscillators. Now let us assume that one of these oscillators is much lighter than the another. In this case we may assume that in the first approximation the light oscillator practically does not disturb the motion of the heavy oscillator, and that the heavy oscillator vibrates according to the law $y(t) = r \sin \omega_0 t$ with the amplitude and frequency being constant. Owing to existence of the coupling between the oscillators, the heavy oscillator will act on the light one as a periodic external force, and we come to the problem of motion of an oscillator influenced by an external periodic force. However, we have to take into account two important points. First, in order to state the problem correctly, we have to introduce some damping, because otherwise the amplitude of vibrations may increase to infinity. Second, the oscillator must be anharmonic, because for the harmonic

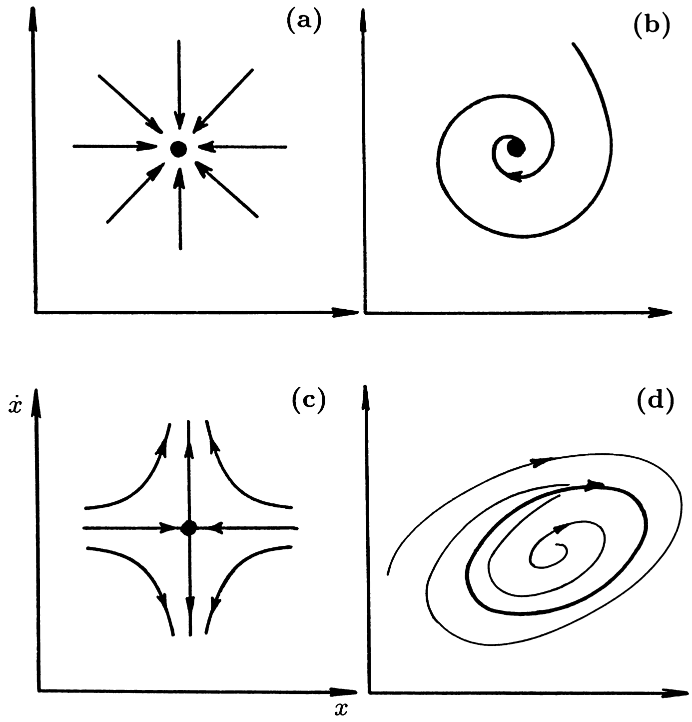

Figure 2.4: Critical points and curves on a plane: (a) the nodal point, (b) the focal point, (c) the saddle point, and (d) the limit cycle.

oscillator the problem is integrable (e.g., see [10]). In the result we come to the *driven pendulum model* which is described by the motion equation

$$\ddot{x} + \eta\dot{x} + \sin x = r \sin \omega_0 t \,, \tag{2.7}$$

where r is the amplitude of the external force and η is the viscous friction coefficient. Introducing the variables $y = \dot{x}$ and $z = \omega_0 t$, Eq. (2.7) can be rewritten as the system of three first-order differential equations

$$\left\{ \begin{array}{lcl} \dot{x} & = & y \,, \\ \dot{y} & = & -\sin x - \eta y + r \sin z \,, \\ \dot{z} & = & \omega_0 \,, \end{array} \right. \tag{2.8}$$

so that the system evolution is described by the trajectory in three-dimensional phase space.

In numerical investigation of the model (2.8) we have to put ω_0 and η to be fixed (e.g., $\omega_0 \sim \eta \sim 1$), and to study the trajectories of system motion for different values of the parameter r which is an analog of the energy parameter of the Hénon-Heiles model.

Recall that in qualitative investigation of dynamics of a dissipative system it is sufficient to find its peculiarities (i.e., to find critical points, curves, surfaces, *etc*). For example, when the system evolution is described by an autonomous second-order differential equation or by the set of two first-order differential equations, the system phase space is a plane, and on this plane only the following peculiarities may exist:

(a) the stable (or unstable) *nodal point* is such a critical point that all phase trajectories approach it (or go away from it) as shown in Fig. 2.4a;

(b) the stable (unstable) *focal point* distinguishes from the nodal point by that in the neighborhood of the focal point all trajectories swirls also (see Fig. 2.4b);

(c) *the saddle point* is such a singular point that two trajectories approach it, while two others go away from it (Fig. 2.4c);

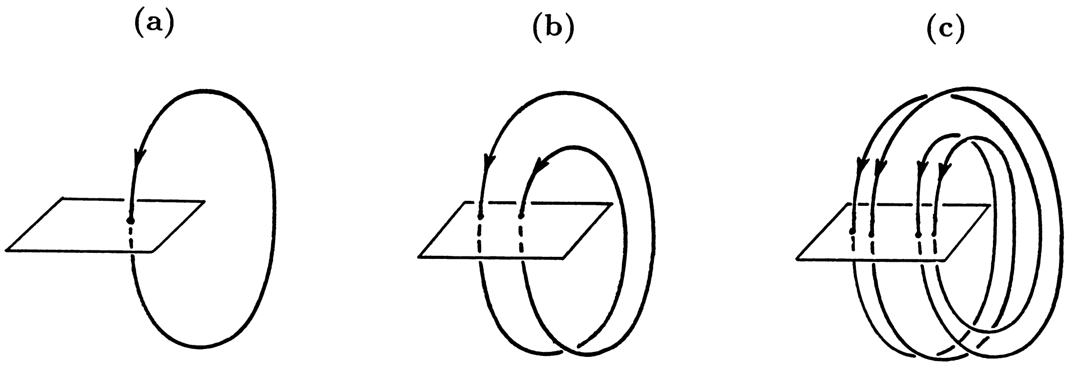

Figure 2.5: Qualitative phase trajectories for the driven pendulum: (a) the single cycle, (b) the cycle of period two, and (c) the cycle of period four.

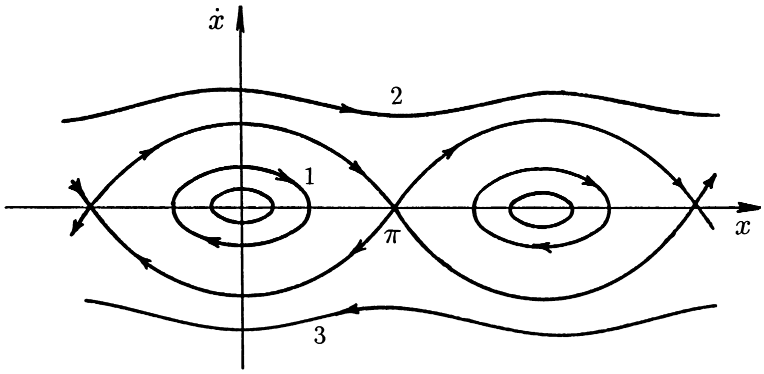

Figure 2.6: Phase portrait of the physical pendulum.

(d) the stable (or unstable) *limit cycle* is the closed trajectory in the phase space such that all trajectories approach it (or go away from it) as is shown in Fig. 2.4d.

When the dimension of the phase space is more than two, there may exist additionally such peculiarities as different kinds of saddle points, limit torus, *etc.* If all trajectories from some neighborhood of the phase space approach to a stable manifold, this manifold is called the *attractor*.

To find the attractor in computer simulation, it is enough to calculate the trajectory of the system motion for a time which is sufficient for the system to reach the attractor. It is convenient to present the results of modeling with the help of the stroboscopic map (an analog of the Poincaré map used for dissipative systems), i.e., to fix the positions of the phase trajectory in discrete time moments $t_n = nT$, $n = 0, 1, 2, \ldots$, which are multiplies of the period of the driven force, $T = 2\pi/\omega_0$. The results of investigation of the driven pendulum (2.7) (see [20]) show that at small amplitude of the external force ($r \ll 1$) the stroboscopic map consists of a single point, i.e., the system attractor is the orbitally stable limit cycle with the period T (see Fig. 2.5a). When the parameter r raises, i.e. when the average energy of the oscillator increases above a certain value, the single point of the stroboscopic map splits into two points (see Fig. 2.5b), i.e. the so-called *period-doubling bifurcation* takes place. With further increasing of r these two points split into four points (see Fig. 2.5c), then into eight points, and so on up to infinity. Finally, at $r > r_{\rm crit}$, where $r_{\rm crit}$ is some critical value, the stroboscopic map corresponds to some set on the $X0\dot{X}$ plane which looks like the stochastic region on the Poincaré map of the Hénon-Heiles model. This set was called the *strange attractor* (Ruelle and Takens [21]).

To make clear the reason why does the chaos emerge, let us consider an isolated physical pendulum, i.e. let us put $r = \eta = 0$ in Eq. (2.7). The phase space for the physical pendulum is shown in Fig. 2.6. The system has two types of stationary states: the vortex points at $\dot{x} = 0$, $x = 2n\pi$, $n = 0, \pm 1, \pm 2, \ldots$, which correspond to the stable states, and the saddle points at $\dot{x} = 0$, $x = (2n+1)\pi$, which correspond to the unstable state of the pendulum at the top position. The ellipses around the vortex points (see curve 1 in Fig. 2.6) describe the pendulum vibrations, while the periodic curves (see curves 2 and 3 in Fig. 2.6), its clockwise or anticlockwise rotations. The regions of the phase space corresponded to these qualitatively different types of system motion, are separated by the peculiar curve called the *separatrix*. The separatrix is the trajectory which connects saddle points. The motion along the separatrix has two essential features. First, this motion is *unstable*, because even the very small external perturbation will move the pendulum either to vibrational regime or to rotational regime depending on the direction of the external force acting on the pendulum when the latter is at the top (unstable) position. Second, the motion along the separatrix takes place for an infinite long time (physically this means that the pendulum "hangs up" at the top position). Thus, when the trajectory of the system motion is too close to the separatrix, it becomes impossible to predict exactly, either even or odd will be the number of half-periods of the external force during one vibration or rotation cycle for the pendulum motion from one top position to the next one. Therefore, we can not predict the direction of the external force at the top position, and, consequently, can not predict the type of the pendulum motion (either rotation or vibration) for the next cycle. Namely this instability of motion in the neighborhood of the separatrix is the reason why the chaotic motion does exist. Therefore, with increasing of the amplitude of the external force r, the amplitude of the pendulum vibrations increases too, and the phase trajectory comes to the vicinity of the separatrix, where the system motion becomes chaotic. For a more detailed investigation of the driven pendulum model which in fact is much more rich and complicated than it has been described above, we can refer to papers [22, 23, 24, 25].

Thus, the driven pendulum model helped us to understand the reason for the appearing of chaotic motion (note that the instability of the system motion in the stochastic regime was shown by Hénon and Heiles in their original paper [19]). But the question on the mechanism of creation of the chaos still remains unanswered, as well as the question of the nature of the chaotic motion itself, i.e. on a structure of the strange attractor. Therefore, it is very desirable to make a further simplification of the model under investigation. For example, let us suppose that the external force does not act continuously but consists of the discrete δ-pulses, i.e., let us put $\sin \omega_0 t \to T^{-1} \sum_{n=-\infty}^{\infty} \delta(t - nT)$ in Eq. (2.7). For this model known as the *periodically kicked rotator model*, the trajectory of system motion between the sequent points of the stroboscopic map can be calculated analytically. However, it will be better to act more radically: let us simply invent a new, more simple model. Namely, let us invent a simple rule, $x_{n+1} = F(x_n)$, with the help of which we can find the $(n+1)$-th point of the Poincaré map from the n-th point. The simplest function $F(x)$ which leads to the chaotic motion, is the square function. In this way we come to the so-called *logistic map*.

Note that the reasoning with the help of which we were going from the three-body problem to the restricted three-body problem, then to the Hénon-Heiles model, then to the driven pendulum model, and finally to the logistic map, should not be considered as the deduction of one model from the another one. New models have to be invented but not deduced, while the reasons given above may only help to find a possible way of thinking.

2.3 Logistic map

Let us consider the following simple one-parameter map of unit interval into itself known as the *logistic map*:

$$x_{n+1} = F(x_n)\,, \quad F(x) = rx(1-x)\,. \tag{2.9}$$

Here the index n plays the role of the discrete time, and the parameter r plays the same role as the amplitude of the external force in the driven pendulum model. To have the problem correctly stated, we also have to define the regions of x and r variation. It is natural to take $x \in (0,1)$; then the variation of the parameter r should be restricted to the interval $1 < r \leq 4$, because otherwise the values of x may go out the limits of the interval $(0,1)$.

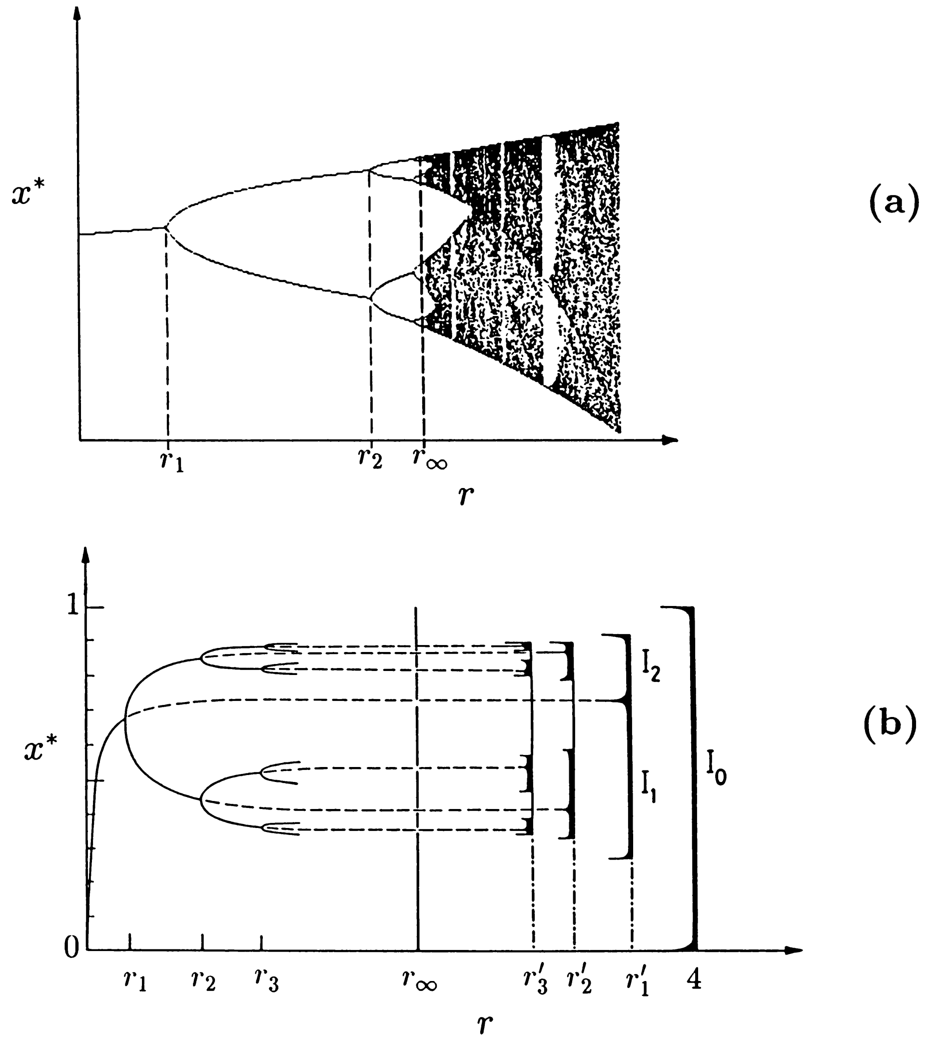

Figure 2.7: Iterates of the logistic map (2.9) (from [14]).

Investigation of the map (2.9) reduces mainly to looking for its attractor x^* for a fixed value of the parameter r. Namely, starting from an arbitrary point x_1, we have to calculate sequently the points x_2, x_3, $\ldots$, and then to find the point (or the set of points) x^* to which the points x_n are approaching at $n \to \infty$. Investigations of the logistic map when the parameter r varies within the interval $1 < r \le 4$, have led to a rather complicated picture [26, 27, 28]. Results of numerical modeling of the map (2.9) are shown in Fig. 2.7. We see that it exists some critical value r_∞ ($r_\infty = 3.5699456\ldots$ for the model (2.9)) such that for $r < r_\infty$ the attractor consists of a finite number of points (one, two, four, *etc*), while for $r > r_\infty$ it contains an infinite number of points, and at $r \to 4$ the attractor occupies the whole interval (0,1), i.e., the whole region where the map (2.9) is defined.

Fortunately, at $r = 4$ the logistic map can be investigated analytically. Namely, using the substitution

$$x_n = \frac{1}{2}(1 - \cos 2\pi\theta_n)\,, \tag{2.10}$$

Eq. (2.9) at $r = 4$ can be transformed to the equation $\theta_{n+1} = 2\theta_n$. Here, however, we must take into account that the values θ and $\theta + i$, where i is an arbitrary integer number, determine the same value of x. Therefore, in order for the transformation (2.10) to be single valued, we must restrict the variation of θ by a unit interval, for example, $0 \le \theta < 1$. Thus, the logistic map for $r = 4$ reduces to the so called *Bernoulli* *shift*:

$$\theta_{n+1} = \{K\theta_n\}, \quad K = 2\,. \tag{2.11}$$

The map (2.11) is nonlinear due to the operation of taking of the fractional part,

$$\{x\} = x - \text{int}(x) = x \,(\text{mod } 1)\,,$$

and it is unstable owing to $K > 1$.

To study the map (2.11), let us start from an arbitrary number θ_1, for example, $\theta_1 = 0.703125\ldots$, and write it in binary (because $K = 2$) representation:

$$\theta_1 = \frac{1}{2} + \frac{1}{8} + \frac{1}{16} + \frac{1}{64} + \cdots = 0.101101\ldots \tag{2.12}$$

The consequent points generated by the map (2.11), are the following:

$$\begin{aligned} \theta_2 &= \left\{1 + \tfrac{1}{4} + \tfrac{1}{8} + \tfrac{1}{32} + \cdots\right\} = \{1.01101\ldots\} = 0.01101\ldots, \\ \theta_3 &= 0.1101\ldots, \\ \theta_4 &= 0.101\ldots, \end{aligned} \tag{2.13}$$

etc. Thus, the operation (2.11) reduces to the shift of the whole number on one bit to the left and to discarding of the integer part when it arises.

Now, if we take as the initial conditions the two close points θ_1 and θ_1' which have, for example, the identical first 100 binary digits but the consequent digits are different, then during the first 100-th steps the trajectories θ_n and θ_n' will be close to one another but, starting from the 101-st step, the points θ_n and θ_n' will separate, and further they will move independently from each other. In other words, even if we set the initial point with the very high precision, there always will occur a moment after which the system evolution will be completely unpredictable. Clearly that in this case the system dynamics is irreversible in time, because in order to have the reversibility we must specify the initial conditions with the infinite accuracy, but this is impossible in principle.

Now let us show why it is natural to name the sequence of point θ_n of the map (2.11) as the chaotic one. Indeed, let us take a chaotic sequence of zeros and ones which can be obtained, for example, with the help of the throwing out a coin, and let us use this sequence as the initial point θ_1. Clearly that the statistical characteristics of the resulting trajectory θ_n will be undistinguishable in principle from the characteristics of the random sequence of the throwing out the coin.

Describing the chaotic dynamics, it is natural to use not a single trajectory $x(t)$ but the probability distribution $\rho(x,t)$. According to the definition, the product $\rho(x,t)\,\Delta x$, where $\Delta x \to 0$, is equal the probability that the system is within the interval $(x, x + \Delta x)$ at time t. Using this definition, we can define chaos in mathematically rigorous way.

(a) The chaos exists in the system, if it exists the *limit probability distribution* (or the *invariant measure*) in the phase space, $\rho_\infty(x)$, such that almost any initial distribution approaches to $\rho_\infty(x)$ at $t \to \infty$.

Sometimes, for very simple systems, the function $\rho_\infty(x)$ can be found analytically. For example, for the logistic map at $r = 4$ we have $\rho_\infty(\theta) = 1$, or $\rho_\infty(x) = 1/\pi\sqrt{x(1-x)}$ (the proof can be found, e.g., in the book [17]). Usually, however, to prove the existence of the limit probability distribution and, all the more, to find it, is the extremely difficult problem, thus we have to use less rigorous statements.

Let $\tilde{f}(x)$ be a function defined in the phase space Γ. Then, if $x(t)$ is a trajectory of the system motion, the function $f(t;x_0) \equiv \tilde{f}[x(t)]$ will depend on time as well as on the initial point $x_0 \equiv x(0)$. Let us define the time averaging as

$$\langle f(t;x_0)\rangle_t = \lim_{T\to\infty} \frac{1}{T}\int_0^T dt\, f(t;x_0)\,. \tag{2.14}$$

Now we can make the following statements:

(b) If the chaos exists in the system, then

(b1) the time average (2.14) exists, and

(b2) it does not depend on the initial condition x_0.

Clearly that in this case the time mean has to coincide with the average over the invariant distribution,

$$\langle f(t;x_0)\rangle_t = \langle \tilde{f}(x)\rangle_\Gamma \equiv \int_\Gamma dx\, \tilde{f}(x)\rho_\infty(x)\,. \tag{2.15}$$

The statement **(b1)** is known as the *ergodic hypothesis*, and the statement **(b2)**, as the *Boltzmann hypothesis*, or the *hypothesis of molecular chaos*.

The simplest way to determine a character of system motion in the computer experiment is to calculate the correlation or spectral functions. The time (self-) correlation function is defined by the relationship

$$Q_f(\tau) = \lim_{T\to\infty} \frac{1}{T}\int_0^T dt\, f(t+\tau)f(t)\,, \tag{2.16}$$

and the spectral function, as its Fourier transformation

$$F_f(\omega) = \frac{1}{2\pi}\int_{-\infty}^{+\infty} d\tau\, e^{-i\omega\tau} Q_f(\tau)\,. \tag{2.17}$$

[Notice two important computational details. First, for the calculation of the function $Q_f(\tau)$ within the interval $0 \le \tau \le \tau_{\max}$ we have to find in advance the function $f(t)$ within the more broad interval $0 \le t \le T + \tau_{\max}$. Second, in calculation the integral (2.17) it is usually convenient to employ the fast Fourier transform. To do this, the time step $\Delta\tau$ should be chosen in a way that the total number of points being equal to 2^m with an integer m.] The following statement is valid:

(c) If the chaos exists in the system, its time correlation function has to decay according to exponential law. More rigorously, there have to exist two constants C and Λ which do not depend on the function f, such that

$$\mid Q_f(\tau) \mid \le C\exp(-\Lambda\tau) \quad \text{for} \quad \tau \to \infty. \tag{2.18}$$

The statement **(c)** is equivalent to the following statement:

(d) If the chaos exists in the system, its power spectrum is "dense", or, more rigorously, the spectral function is absolutely continuous.

Emphasize that the statements **(a)** and **(b)** are the necessary and sufficient conditions, while the fulfilment of the conditions **(c)** and **(d)** is necessary but not sufficient for existence of chaotic dynamics.

From the described above investigation of the logistic map it is clear that in order for the chaos to exist, two conditions must be fulfilled: first, the phase space must be continuous (in the discrete phase space the dynamical chaos cannot exist) and, second, the motion equations must have an instability. Owing to the first condition the initial conditions will always have some microscopic uncertainty, because it is impossible to specify the position of the initial point with the infinite accuracy (the infinite accuracy needs the infinite body of information). Due to the second condition the deterministic motion equations "unwrap" this microscopic initial uncertainty into the macroscopic uncertainty of the trajectory of the system motion.

The attractor of the map (2.11) fills the whole region where the map is defined. Within the interval (0,1) the chaotic trajectories form the manifold of the uncountable cardinality, namely, the class of all irrational numbers. Thus, if we take as the initial condition a point from the interval (0,1) in a random way, we will obtain with the probability one an irrational number which will lead to the chaotic trajectory. At the same time, this attractor contains the infinite (but countable) set of rational numbers, and each rational number will lead to the regular periodic trajectory.

Thus, the investigation of the logistic map allows us to achieve the main goal of modeling, namely to simplify the model to such a degree that it becomes possible to explain the phenomenon under investigation "by fingers". Additionally it allows us to understand not only the nature of the dynamical chaos, but, as will be shown in the next Sec. 2.4, also the mechanism of the transition from the regular to chaotic motion.

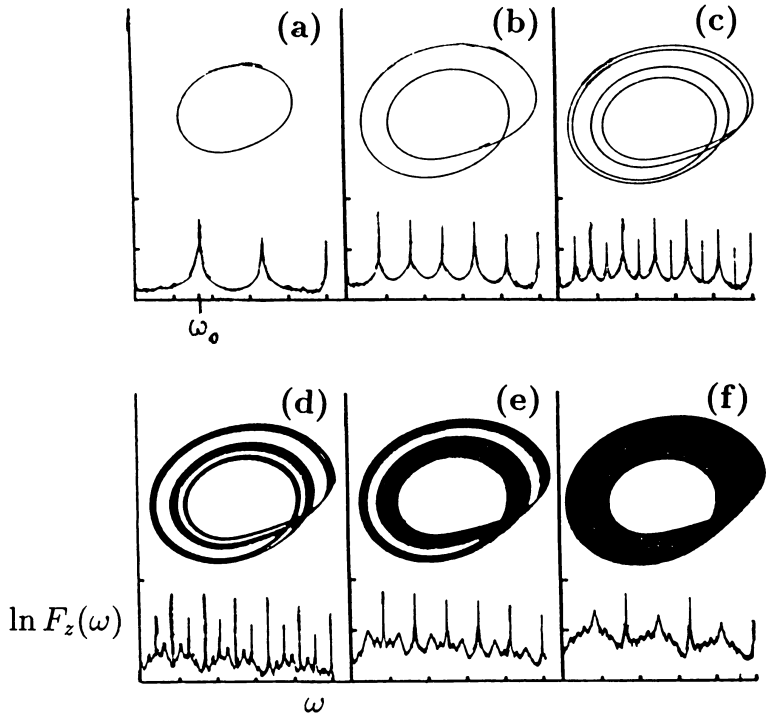

Figure 2.8: Period-doubling bifurcations for the Rössler attractor (2.22) as projected onto the $X0Y$ plane at (a) $r = 2.6$, (b) $r = 3.5$, (c) $r = 4.1$, (d) $r = 4.23$, (e) $r = 4.30$, and (f) $r = 4.60$ as calculated in [29]. The corresponding power spectral density of $z(t)$ is shown in the down parts of the figures.

2.4 Feigenbaum theory

Scenario of the transition from the regular to chaotic motion with the increase of the parameter r is clear from Fig. 2.7. At small r, $r < r_1$ ($r_1 = 3$ for the logistic map), the attractor consists of the single point x^* which is the stable solution of the equation

$$x = F(x)\,. \tag{2.19}$$

[The solution x^* is known as the *fixed point* of the map (2.9). The fixed point x^* is stable if $|F'(x^*)| < 1$.] In a real physical system this situation corresponds to existence of the orbitally stable limit cycle with the period $T = T_0$, and the Fourier spectrum of the system consists of the single harmonic with the frequency $\omega = \omega_0$ (see Fig. 2.8a). Recall that the parameter r of the map (2.9) plays the similar role as the amplitude of the external force in the driven pendulum model or the total energy in the Hénon-Heiles model. With r increasing above the point $r = r_1$, the so-called *period-doubling*, or *pitchfork bifurcation* takes place. Namely, at $r > r_1$ the solution x^* of Eq. (2.19) becomes unstable, i.e. for two sequential points of the map, $x_n = x^* + \Delta x_n$ and $x_{n+1} = x^* + \Delta x_{n+1}$, we now have $|\Delta x_{n+1}| > |\Delta x_n|$. However, instead of the single critical point x^*, there emerge two new points x_1^* and x_2^* which are solutions of the equation

$$x = \tilde{F}_2(x) \equiv F(F(x))\,. \tag{2.20}$$

This solution is stable within the interval $r_1 < r < r_2$, where $r_2 = 3.4495\ldots$ for the map (2.9). In a real physical system the period-doubling bifurcation corresponds to the "splitting" of the limit cycle (see Fig. 2.8b) so that in a result the period of the new limit cycle becomes equal $T = 2T_0$, and the new harmonic with the frequency $\omega = \frac{1}{2}\omega_0$ appears in the frequency spectrum. With further increasing of r at $r = r_2$ the next period-doubling bifurcation takes place (see Fig. 2.8c), then, at $r = r_3$, the next bifurcation, and so on up to the value $r = r_\infty - \delta$ (where $\delta \to 0$) when the attractor becomes to be consisting of the infinite (countable) number of points, and the frequency spectrum, of the same number of harmonics.

With r increasing in the region $r > r_\infty$, the isolated points of the attractor "broadens" to small intervals which then sequentially merge with each other (see Fig. 2.7). In the previous Sec. 2.3 we have shown that at $r = 4$ the attractor of the logistic map takes the whole interval from 0 to 1 (see Fig. 2.8f). When r decreases starting from the $r = 4$ value, the interval occupied by the attractor shrinks, and at $r = r'_1$ the so-called *inverse period-doubling bifurcation* takes place, so that the "blob" of trajectories splits into two more narrow "blobs", or "branches". Within the region $r'_2 < r < r'_1$ the attractor consists of two "branches" as is shown in Fig. 2.8e, the each second point of the stroboscopic map belongs to the same subregion of the strange attractor (i.e., to one of the "branches") and fills it randomly, while the sequential points of the map change the "branches" in the regular way. At the same time, in the frequency spectrum which was dense for $r > r'_1$, at $r < r'_1$ the discrete harmonic with the frequency $\omega = \frac{1}{2}\omega_0$ appears, and the amplitude of the continuous contribution decreases (see Fig. 2.8e). At $r = r'_2$ the next inverse period-doubling bifurcation takes place, the "branches" of trajectories split again so that the attractor becomes consisting of four "branches", and the new harmonics with the frequencies $\omega = \frac{1}{4}\omega_0$ and $\omega = \frac{3}{4}\omega_0$ appear in the frequency spectrum (see Fig. 2.8d). With further r decreasing, an infinite number of inverse period-doubling bifurcations takes place so that at $r = r_\infty + \delta$ ($\delta \to 0$) the attractor becomes consisting of the infinite (countable) number of infinitely narrow intervals, and this attractor then matches with the attractor consisting of the same (infinite) number of isolated points at $r = r_\infty - \delta$.

Calculating with the help of a pocket calculator the values of the parameter r_i, $i = 1, 2, \ldots$, at which the period-doubling bifurcations take place, Feigenbaum [30] discovered that the values r_i approximately produce a geometric progression. (Interesting that, according to the Feigenbaum paper [31], namely the absence of a possibility to use a high-speed computer helps to discover this phenomenon.) Namely, the sequential bifurcation points are subject to the law

$$\lim_{i\to\infty} \frac{r_{i+1} - r_i}{r_i - r_{i-1}} = \frac{1}{\delta}, \quad \text{or} \quad (r_\infty - r_i) \propto \delta^{-i}, \tag{2.21}$$

where $\delta = 4.6692016091\ldots$ Later, investigating (again with the help of a calculator) the another one-dimensional map $x_{n+1} = r \sin \pi x_n$, Feigenbaum discovered that the bifurcation points again produce the geometric progression, and with the same common ratio δ! Moreover, the sequence r'_i of the inverse period-doubling bifurcations follows the law (2.21) too! Thus, the results of computer modeling suggest that the law (2.21) has a general character. Indeed, with the help of the renormalization-group technique Feigenbaum proved ([32], see also [33]) that the law (2.21) is satisfied for any one-dimensional map of an interval into itself, $x_{n+1} = F(x_n)$, provided the function $F(x)$ has a single maximum within the interval where the map is defined (a more detailed description of the Feigenbaum theory may be found, e.g., in [17]).

Above we have tried to show that the maximum simplification of the model is the necessary condition for the modeling to be successful. However, at the next stage of modeling we have to turn back to reality. In other words, further we should complicate the model in order to become sure in invariability of the founded laws as well as to establish whether new effects would appear. With the help of computer modeling it has been shown that the driven pendulum model as well as a majority of other nonlinear dissipative systems show the transition to chaos according to the same scenario described above. In particular, the trajectories and Fourier spectra showed in Fig. 2.8, were calculated in the work [29] for the system of equations

$$\begin{cases} \dot{x} &= -y - z\,, \\ \dot{y} &= x + \frac{1}{5}y\,, \\ \dot{z} &= \frac{1}{5} - rz + xz\,, \end{cases} \tag{2.22}$$

where r is the external system parameter. This model was introduced by Rössler [34, 35] in order to describe dynamics of chemical reactions which take place in a vessel with mixing. The attractor for the Rössler model is shown in Fig. 2.9. From this figure it is easy to see why the existence of dynamical chaos needs $1\frac{1}{2}$ degrees of freedom, i.e. the motion of the system must take place in three-dimensional phase space as minimum. Indeed, owing to existence of the instability, the close phase trajectories diverge, i.e. the trajectory spirals away from the critical point (unstable focal point). However, first, the trajectory cannot get out from the

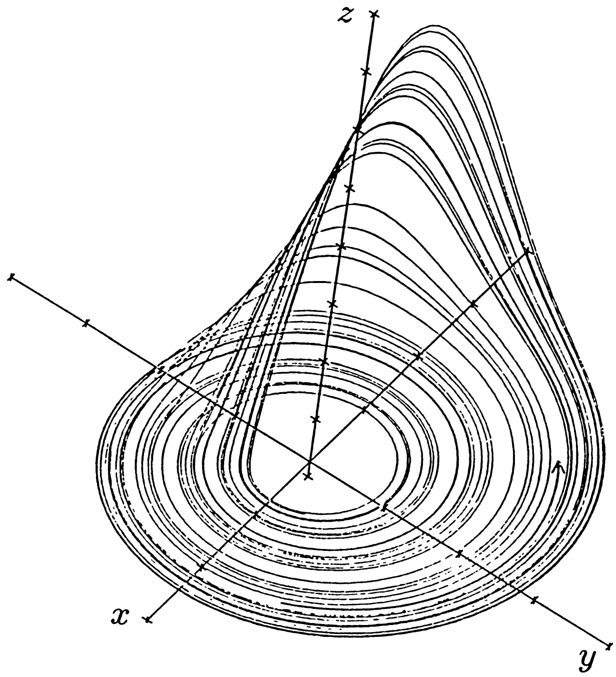

Figure 2.9: The Rössler attractor as calculated in [29].

attractor, i.e. from the bounded region of the phase space, and, second, according to Cauchy's theorem the phase trajectories cannot be intersected. Therefore, if the "untwisting" of the trajectory took place on some two-dimensional surface, then the trajectory must "go out" to a third dimension of the phase space in order to return to the vicinity of the unstable critical point.

Such a broad applicability of the Feigenbaum theory can be explained in the following way. As is known, for a dissipative system the phase volume taken by the system, must shrink as time increases. Therefore, the phase trajectories must crowd together in average. However, for the existence of an instability the nearest trajectories must diverge. These two conditions may be satisfied simultaneously, if the trajectories lying on one hypersurface, diverge, while the trajectories which belong to the orthogonal hypersurface, crowd together (see Fig. 2.10), and in average the latter exceeds the former. If the hypersurface where the phase trajectories diverge, is a two-dimensional surface (and namely such a situation takes place in a number of physical systems), than the transition to chaos in this system should be described by the Feigenbaum theory independently on the total dimensionality of the phase space.

2.5 Strange attractor

Investigation of chaotic dynamics in a dissipative system reduces mainly to looking for its strange attractor. The structure of the strange attractor is rather interesting [36, 37] (see also a review [38]). First, it occurs to be within a "sack", i.e. within a closed region of the phase space, so that each trajectory which came into the sack, cannot escape from it. Second, within the sack, only the unstable critical points exist. For example, the Rössler attractor has the single unstable focal point (see Fig. 2.9). The another well known attractor is the attractor of the Lorenz model shown in Fig. 2.11. This model was introduced by Lorenz [40] for the very simplified (three-mode) description of motion of viscous uncompressed fluid confined into a box with the heated bottom, where the Rayleigh-Bénard convention has to arise with increasing of the temperature difference between the bottom hot surface and the top cold surface. The Lorenz model is described by the

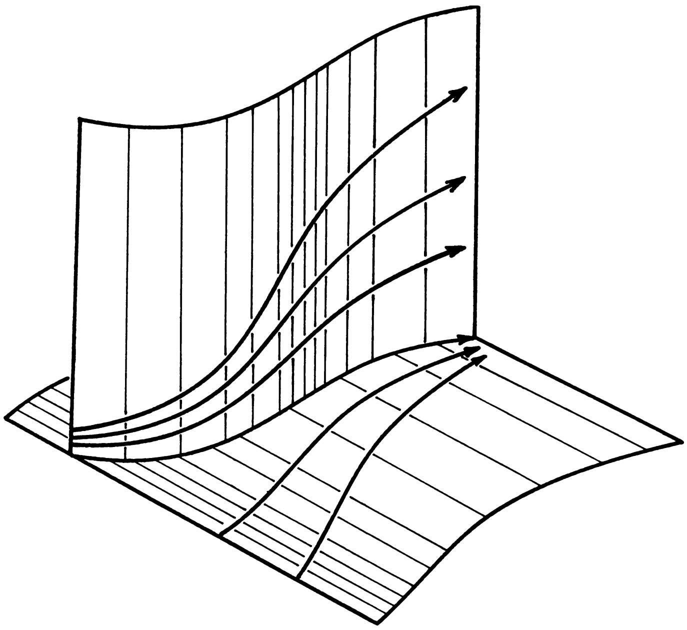

Figure 2.10: Qualitative behavior of phase trajectories on different (hyper-) surfaces.

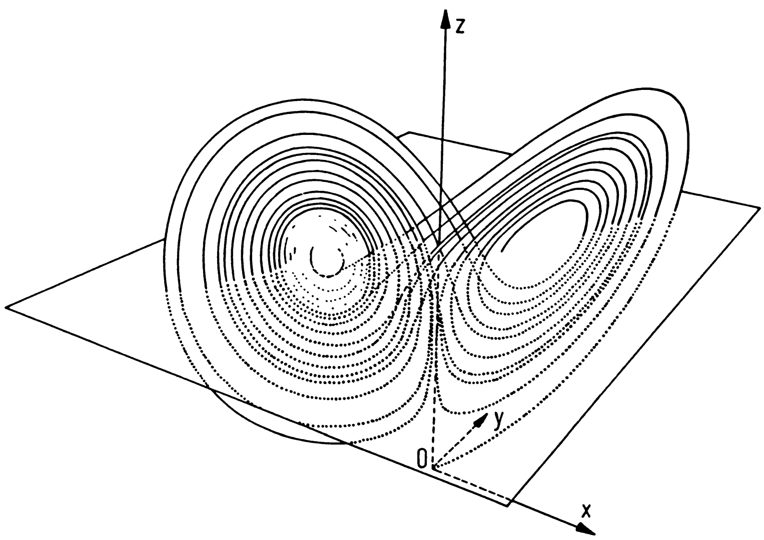

Figure 2.11: The chaotic trajectory for the Lorenz attractor at $r = 28$ as calculated by Lanford [39].

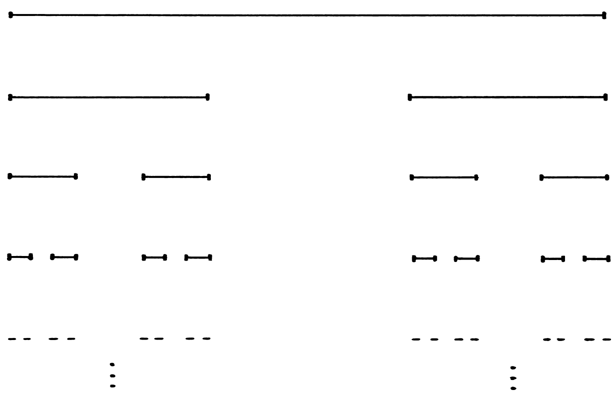

Figure 2.12: Sequent steps of construction of the "middle-thirds" Cantor set.

system of equations

$$\begin{cases} \dot{x} &= -10x + 10y\,, \\ \dot{y} &= rx - y - xz\,, \\ \dot{z} &= -\frac{8}{3}z + xy\,. \end{cases} \tag{2.23}$$

Here r is the control parameter known as the Rayleigh number. In the sack of the Lorenz model at $r > 24.74$ there exist one saddle point and two unstable focal points, so that the trajectory within the sack has to "rush about" between the unstable critical points (that reminds the children game "fifth angle"), asymptotically approaching to the strange attractor.

Because an elementary phase volume of the dissipative system should decrease with time evolution, the dimension of the strange attractor d must be lower than the dimension of the original phase space ν. Besides, at least in one direction of the phase space the strange attractor should have the structure of the Cantor set. A simplest way to explain the structure of the Cantor set, is to describe the concrete example of the "middle-thirds" set. Namely, let us take the closed unit interval, divide it into three parts and delete the middle open (i.e., excluding the end points) part as is shown in Fig. 2.12. Then let us divide each of the remaining intervals into three parts, and delete the middle parts again. Repeating this procedure by the infinite number of times, in what leaves we finally obtain the set with the structure of the Cantor set. It is characterized by the following properties:
(a) The Cantor set has the zero Lebesgue measure. Indeed, the "length" of the "middle-thirds" set is equal $1 - (\frac{1}{3} + 2\frac{1}{3^2} + 2^2\frac{1}{3^3} + \cdots) = 0$.
(b) The Cantor set is uncountable, because it contains "the same number" of points as the original unit interval. Indeed, at each step of construction of the "middle-thirds" set, it contains the uncountable number of points, therefore the limit set should have the same cardinality number as the set of irrational numbers.
(c) The Cantor set is totally disconnected, and it is *scale-invariant* (sometimes the terms "self-similar" or "auto-modeling" are used). Crude speaking, considering this set with a "microscope", we will see the same picture at any magnification. The scale invariance of the "middle-thirds" set is clear from its construction, because each next step of construction has repeated the previous one.

A fine model of the strange attractor has been proposed by Hénon [41]. The Hénon model is the two-dimensional discrete map of a rectangular into itself described by the set of equations

$$\begin{cases} x_{n+1} &= y_n + 1 - 1.4x_n^2\,, \\ y_{n+1} &= 0.3x_n\,. \end{cases} \tag{2.24}$$

Equations (2.24) were chosen in such a way that to describe approximately the Poincaré map for the Lorenz model (2.23). In constructing the strange attractor we may start from an arbitrary point and then remove few first points (about ten or hundred points). The results of numerical investigation of the model (2.24) are

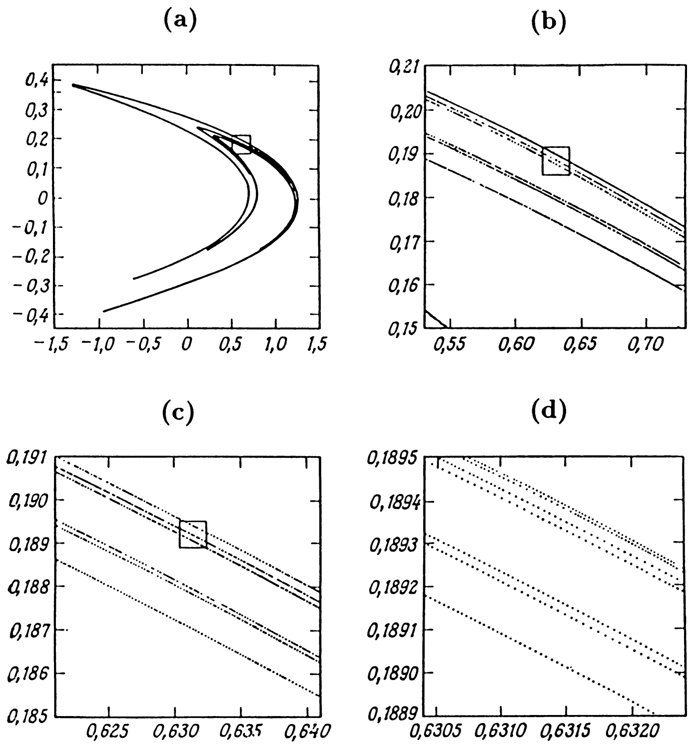

Figure 2.13: Layered structure of the Hénon attractor as calculated in [41]. (a) The whole attractor, (b) to (d) enlargements of the squares in the preceding figure.

shown in Fig. 2.13. The whole strange attractor of the Hénon model is plotted in Fig. 2.13a. Figure 2.13b scales up the part of the attractor which is inclosed in the small square in Fig. 2.13a. The small square of Fig. 2.13b is scaled up in Fig. 2.13c, and the small square of Fig. 2.13c, in Fig. 2.13d (note that in the numerical experiment the each "magnification" is to be followed by the increase of the total number of computed points in the same times). As seen, for any magnification the structure of the strange attractor remains the same: it consists of a series of continuous curves, while in the direction perpendicular to the curves, it has the structure of the Cantor set. Analogously, the strange attractor of dissipative systems described by continuous differential equations, has the structure of the Cantor set on the hypersurface where the nearest trajectories diverge (the vertical surface in Fig. 2.10) in the directions perpendicular to the trajectory.

A quantitative characteristic of the strange attractor is its *fractal*, or *Hausdorff dimension.* It is determined in the following way. In the ν-dimensional phase space of the system under consideration let us take small cubes with a size ϵ, i.e. with the volume ϵ^ν, and cover by them the strange attractor. Let $M(\epsilon)$ is the minimum number of cubes needed to cover the whole attractor. Then the fractal dimension (sometimes known as the *capacity*) is defined by the relationship [42] $M(\epsilon) \propto \epsilon^{-d}$, or

$$d = -\lim_{\epsilon \to 0} \frac{\ln M(\epsilon)}{\ln \epsilon}\,. \tag{2.25}$$

For example, for the the "middle-thirds" set the fractal dimension is equal $d = \ln 2/\ln 3 \approx 0.631$, for the logistic map at $r = r_\infty$, $d \approx 0.548$, for the Hénon attractor $d \approx 1.26$, for the Rössler attractor $d \approx 2.01$, and for the Lorenz attractor $d \approx 2.06$ [43, 44]. In computer experiments, however, the calculation of d is a rather difficult procedure, but it is relatively simple to find the Liapunov exponents λ_i, $i = 1, \cdots, \nu$ [44]. Recall that $\sum_{i=1}^{\nu} \lambda_i < 0$ for the dissipative system, and that at least one of the Liapunov exponents must be positive when an instability exists. Let λ_i are numerated in the decreasing order, $\lambda_1 > \cdots > \lambda_s > 0 > \lambda_{s+1} > \cdots > \lambda_\nu$,

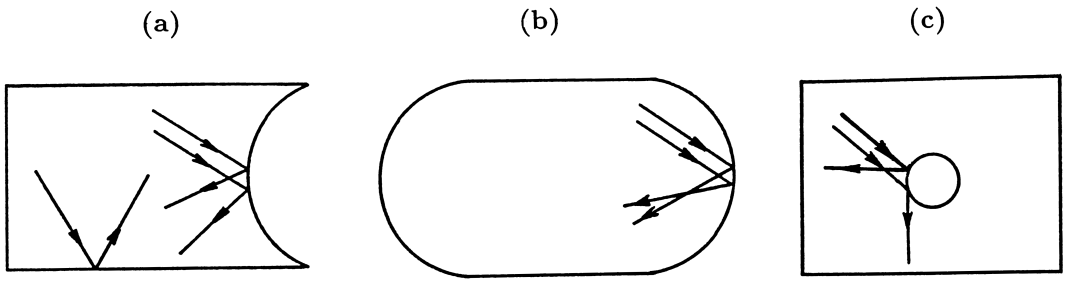

Figure 2.14: The Sinai billiards.

and let m is such an integer that

$$\lambda_1 + \lambda_2 + \cdots + \lambda_{m-1} > 0\,, \tag{2.26}$$

but

$$\lambda_1 + \lambda_2 + \cdots + \lambda_{m-1} + \lambda_m < 0\,. \tag{2.27}$$

Then let us choose the value α $(0 < \alpha < 1)$ from the condition

$$\lambda_1 + \lambda_2 + \cdots + \lambda_{m-1} + \alpha\lambda_m = 0\,. \tag{2.28}$$

According to the Kaplan-Yorke conjecture [45] which was confirmed by computer experiments, the fractal dimension d is very close to the *information dimension* d_{KY}:

$$d \approx d_{KY} = m + \alpha\,. \tag{2.29}$$

Other methods of calculation of the fractal dimension as well as characteristics of the strange attractor which are coupled with the former, can be found in [46] as well as in Part 6 of Moon's book [47].

2.6 Kolmogorov-Sinai entropy

Now let us return to conservative systems. The simplest among the conservative models with two degrees of freedom is the Sinai billiards, or stadium shown in Fig. 2.14. It describes the frictionless motion of a ball (more exactly, a disk) on the limited from all sides plane, and reflections from the boundaries are carried out according to the law "the reflection angle is equal to the incidence angle". In some cases, for example, when the billiards has the rectangular or round shape, the system is exactly integrable because it splits into two independent subsystems, each having one degree of freedom. However, if at least one of the walls is concave, Fig. 2.14a, or convex as in Fig. 2.14b, then the system dynamics becomes stochastic (according to the established terminology, in dissipative systems the word "chaotic" is commonly used, while in conservative systems the name "stochastic" is more often used). The instability which is responsible for arising of chaos, may be clarified from Fig. 2.14a: two neighboring trajectories being parallel before the collision with the concave wall, after the collision begin to diverge. It is clear that, analogously, the dynamics of the billiards with a "hole" in the middle will be stochastic too (Fig. 2.14c), as well as if instead of the "hole" we put the second immobile ball, or if two, or three, or many balls run over the billiards simultaneously. By the way, the last of the mentioned models is known as the *Lorenz gas*, and up to now it is the unique model where the validity of statistical physics laws is proved strictly mathematically [48, 49].

Simplicity of dynamics of the Sinai billiards is caused by that there are no islands of stability in this model, the stochastic trajectories occupy the whole phase space, and the "measure of chaos" does not depend on the system energy. Usually, however, the behavior of conservative systems is more complicated than that of dissipative ones. Excluding exotic cases such as the Sinai billiards, there always exist islands of stability (*invariant tori*) where the motion is regular [this statement is known as the KAM theorem

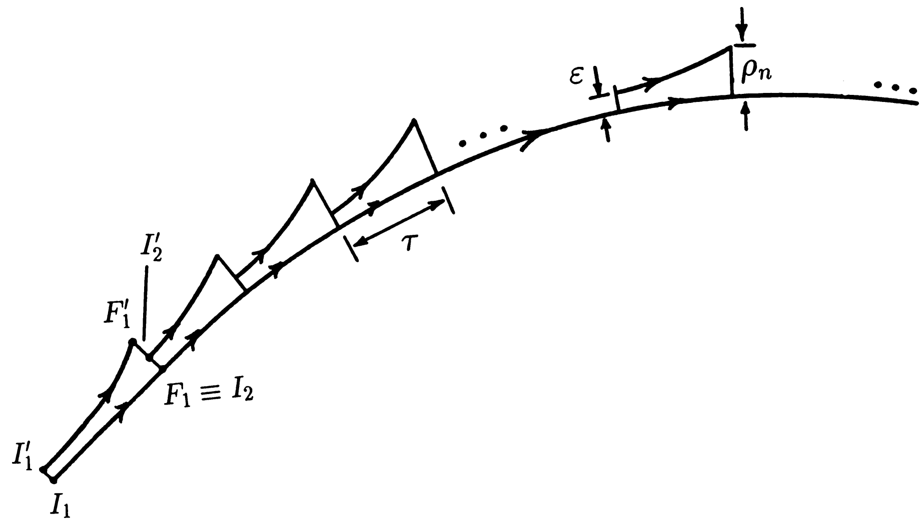

Figure 2.15: Numerical calculation of the maximal Liapunov exponent (after Benettin *et al.*[57]).

(Kolmogorov [50], Arnold [51], and Mozer [52])]. At small value of the total energy E of the system these islands occupy almost the whole available phase space, being separated from each other by thin stochastic layers. This regime is known as the *undeveloped* (or *local*, or *isolated*, or *weak*) stochastic regime. With increasing of the energy E the measure of these stochastic layers increases, and at some critical energy E_{crit} the neighboring stochastic layers overlap. (To estimate analytically the critical energy E_{crit}, it is convenient to use the Chirikov criterion [53, 54, 55] known as the *resonance overlap criterion.* It is described in detail in, e.g., the books [14, 16]). For $E > E_{\text{crit}}$ the *developed* (or *global*, or *connected*, or *strong*) chaos emerges in the system, and stochastic trajectories occupy a majority of the phase space, although small islands of stability continue to exist at any system energy. Thus, opposite to dissipative systems, in the conservative system the transition from the undeveloped chaos to the developed chaos is smooth. Ii is interesting that this transition is also described by the Feigenbaum theory, but with another common ratio δ of the geometric progression (for conservative systems $\delta = 8.72\ldots$).

A method of investigation of stochastic dynamics, most often used in computer experiments, is to calculate the Poincaré map, especially when the section plane is chosen "successfully". (In a general case instead the section plane we may introduce the so-called "surface without contact", i.e. a smooth surface which is intersected without touching in all its points by the phase trajectory.) The computation of correlation functions and Fourier spectra is useful too. But to estimate quantitatively the "measure of chaos" in the system, we have to calculate the so-called *Kolmogorov-Sinai* (KS) *entropy* h which characterizes the rate of diverging of neighboring trajectories. To find h numerically (see [56, 57]), we have to calculate simultaneously two trajectories, the main trajectory (called also the "reference" trajectory) and the "shifted" trajectory as is shown in Fig. 2.15. The total simulation time interval $t_{\max}$ is divided into N_τ small fixed intervals τ. Let the main trajectory starts at some point I_1 of the phase space. Then the point I_1' which defines the initial conditions for the "shifted" trajectory, is obtained from the point I_1 by its shift in some direction on a value ε. The shift may be done in an arbitrary direction, because the necessary direction will be installed automatically during the simulation process. Then both trajectories are calculated during the time τ. Let the main trajectory comes to the point F_1 for the time τ, and the shifted trajectory, to the point F_1' (Fig. 2.15). Denote the length of the vector $\overline{F_1 F_1'}$ by ρ_1. For the next time interval, $\tau \leq t \leq 2\tau$, the initial points I_2 and I_2' are chosen in the following way: for the main trajectory we take $I_2 = F_1$, and for the shifted trajectory the initial point I_2' is obtained from the point I_2 by its shift on ε in the direction of the vector $\overline{F_1F_1'}$. The described procedure is repeated by N_τ times, and then the following value is calculated:

$$\lambda(I_1, \varepsilon, N_\tau) = \frac{1}{\tau N_\tau} \sum_{i=1}^{N_\tau} \ln\left(\frac{\rho_i}{\varepsilon}\right). \tag{2.30}$$

To define the KS entropy strictly mathematically, we must also take the limits $\varepsilon, \tau \to 0$ and $t_{\max}, N_\tau \to \infty$. In computer experiment, however, numerical parameters ε, τ and N_τ should be chosen in such a way that at their variation in some limits (e.g., when they increase as well as decrease in two or three times) the value λ is to be approximately unchanged. Usually they are taken to be $\varepsilon \sim 10^{-5} \div 10^{-3}$, $\tau \sim 0.1 \div 1$ and $N_\tau \sim 10^3 \div 10^4$ in units which are natural for a given problem [56, 57, 58]. From the procedure described above it is clear that $\lambda(I_1)$ is the maximal Liapunov exponent averaged over the given trajectory. If the initial point I_1 is chosen within the limits of the island of stability, it should be $\lambda(I_1) = 0$; otherwise $\lambda(I_1) = \lambda_c > 0$ and $\lambda(I_1)$ should be independent on the choice of the initial point I_1 within the stochastic region. For the system with two degrees of freedom the KS entropy is determined from $\lambda(I_1)$ with the help of averaging over the position of the initial point within the available phase space [60], $h = \langle\lambda(I_1)\rangle_{I_1}$, or

$$h = \lambda_c \mu\,, \tag{2.31}$$

where μ is the measure of the stochastic region which may be estimated as $\mu \approx A_c/A$, A_c is the area of the region of the Poincaré map occupied by the stochastic trajectory, and A is the total area of the region which is available for the given energy of the system [58]. When the number of degrees of freedom is more than two, the KS entropy is determined by the relationship [59, 60]

$$h = \langle \sum_{\lambda_i > 0} \lambda_i \rangle, \tag{2.32}$$

so that we have to calculate all positive Liapunov exponents [61, 62]. Note, however, that the value h determined by the expression (2.31), leads to sufficiently reliable characteristic of the chaos for many-dimensional systems too.

Thus, the distance between the neighboring trajectories increases in average exponentially fast according to the law $\rho(t) \propto \exp(ht)$. If the system is exactly integrable, we have $h = 0$; otherwise $h > 0$ always. Until the chaos is undeveloped, the value h is small, but when the system energy E excesses the critical value E_{crit}, the KS entropy increases sharply (usually to a value $\sim 10^{-2}$). “Maximal” chaos with the KS entropy $h = \infty$ corresponds to the Markov process. (Note that adaptation the name “entropy” to h is connected with the fact that the KS entropy as well as the Liapunov exponents define an average loss of information on the initial conditions during the system evolution and, therefore, h is closely coupled with Shannon’s information entropy; see detail in, e.g., [17]).

Describing the driven pendulum model we have noted that the motion becomes unstable if it takes place in a neighborhood of the separatrix. In the conservative system the stochastic layers arise near separatrices too; namely, they arise in the region of the intersection of two different separatrices (more rigorously, the intersection of the stable and unstable saddle manifolds). If these separatrices intersect one time at least, they must intersect an infinite number of times, and they create the so called *homoclinic structure* as shown in Fig. 2.16. The stochastic layers emerge namely in the region of the homoclinic structure. (Note that the strange attractor in the dissipative system arises in the region of attraction of the homoclinic structure too). In analytical approach, the homoclinic structure is often looked for with the help of the Melnikov method [63] (see also [64]).

2.7 Conclusion

Thus, the study of chaotic dynamics raises two main questions: first, what is the mechanism of the transition from regular to chaotic regimes of motion, and second, how to describe the system dynamics in the

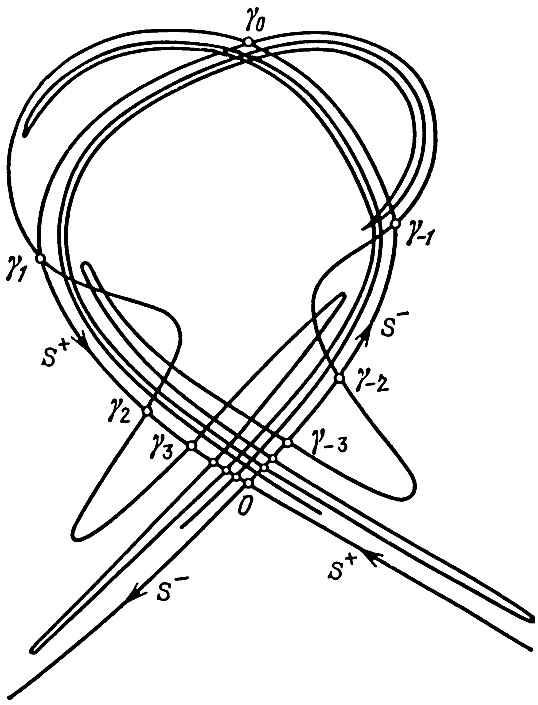

Figure 2.16: Section of the homoclinic structure. $S^{\pm}$ are the separatrices, γ_n $(n = 0, \pm 1, \ldots)$ are the intersection points.

chaotic regime. The transition to chaos usually proceeds thought the infinite sequence of period-doubling bifurcations. In computer or laboratory experiment in this case it will be enough to find few first bifurcation points only, and then the further system behavior can be predicted with the help of the Feigenbaum theory.

However, another scenarios of the route to chaos exist as well. In particular, in the mechanism of route to chaos thought *intermittency*, the regular system motion begins to be interrupted by short chaotic bursts when the control parameter r increases [65, 66, 67, 68]. At the beginning, the chaotic bursts are short and occur rarely, but with r increasing the system spends more and more time in the chaotic regime until the intervals with the regular system motion disappear at all. For example, the transition from regular to chaotic regimes through intermittency was observed in the Lorenz model (2.23) when the parameter r was increased in the interval $166 \leq r \leq 167$ [67].

Another important mechanism of the transition to chaos, the so-called "severe" (sharp? rigid?) mechanism, was observed, for example, in the Lorenz model (2.23) too with increasing of the parameter r from 1 to $24.74\ldots$ (When the parameter r decreases starting from infinity, the chaos in the Lorenz model arises according to the Feigenbaum scenario.) Namely, at small r, $1 < r < 13.926\ldots$, the system behavior is regular, and there are one saddle and two stable focal points in the system. At $r = 13.926\ldots$ the homoclinic trajectories arise (i.e., the two trajectories, the first going out and the second going into the saddle, are united into one closed trajectory), which surrounds the stable critical points. With the further increase of r, the homoclinic trajectories are transferred into unstable limit cycles, the radius of these cycles decreases, and at $r = 470/19 \approx 24.7368$ the cycles collapse into points, absorbing the stable focal points and creating the unstable focal points in the same places.

For the complete description of the system motion in the chaotic regime we have to find the corresponding homoclinic structure in the case of the conservative system, or the strange attractor for the dissipative system. In solution of this problem the computer modeling usually plays the main role. Note also that with the change of the system parameters, the structure of the chaotic manifold may change as well, i.e., the chaos $\rightarrow$ chaos transitions may take place. For example, even in the simplest model such as the logistic map (2.9), within the region $r_\infty < r < 4$ there exist "windows" with the regular dynamics. In particular, with r variation starting from the value $r_c = 1 + \sqrt{8}$, the transition from the regular to the chaotic regime takes place, and in the case of r decreasing this transition is carried out by the intermittency mechanism.

Note also that the structure of the chaotic manifold is "stable", i.e. it remains unchanged under the action of small external perturbations, e.g., a small-amplitude external noise.

In conclusion note that in physics for a long time it has been wide-spread a mistake that any problem of classical mechanics has, at least in principle, the exact solution, and the only problem is to have a sufficiently high-speed computer for its solution. This mistake was based on the fact that in the linear approximation, indeed, any problem is exactly integrable. Of course, there exist a number of nonlinear models which are exactly integrable too (for example, even the Hénon-Heiles model (2.2) is integrable for some particular sets of the parameters such as $\omega_y = 1$ and $\mu = 1/3$, or $\omega_y = 4$ and $\mu = 16/3$, or $\mu = 2$ and arbitrary ω_y), and these models play an extremely important role in physics (see below Chapter 6). It occurs, however, that when a nonlinearity is taken into account, almost all systems are nonintegrable, i.e. they have no analytical solution in an integral form in principle, and their dynamics is chaotic. When this fact has became clear, the stochastic theory spreads over practically all branches of physics as well as of adjacent sciences. In particular, we may give the following examples (much more enormous list of applications of the stochastic theory can be found in Moon's book [47]):

1. *Statistical mechanics.* The stochastic theory put the base for the main hypotheses of statistical mechanics, namely for the ergodic hypothesis (which implies that the time average exists, and it has to coincide with the average over the phase space), and Boltzmann's hypothesis (which states that the average kinetic energy is to be equally shared among all degrees of freedom of the system). It appears that in order these hypotheses to be true, it is not necessary to have an enormous (10^{23}) number of atoms as it was assumed earlier, but it is enough to have a single atom only as in the Sinai billiards! But it does be necessary to have an instability. The instability is also responsible for the time irreversibility of statistical mechanics laws which naturally emerges when the "rough" distribution function is used, i.e. when we reject the attempts to put the initial conditions with the infinite accuracy. At the same time, however, we are losing the configurations which have an extremely small probability to occur (for example, that all gas molecules come together in one half of a volume at a given time moment).

2. *Meteorology.* The Lorenz model (2.23) appears namely in this field of science. In particular, the stochastic theory shows senseless of attempts to predict a weather for a long time period by solution of deterministic motion equations for the atmosphere. The latter approach can predict the weather for a period of $\Delta t \sim \lambda_{\max}^{-1}$ only, this period is about two weeks.

3. *Aero- and hydrodynamics.* A great hope has been put on that the stochastic theory would help to describe the transition from a laminar to the turbulent motion of liquid or gas as well as to describe characteristics of the turbulence regime itself.

4. *Radiotechnique.* When an information is transferred along a line or optical fibre, it is desirable that the noise produced by the line itself and then introduced into the signal, is reduced to a minimum. To achieve this goal, we have to choose the line parameters in such a way that the system has to be as close as possible to the exactly integrable system, i.e. the line has to be characterized by the minimal KS entropy. The corresponding example will be presented in Chapter 6.

5. *Optics.* Lasers with smoothly varying frequency have a large area of application. One of methods to construct such a laser is to make the wideband (noise) laser and then to subtract the necessary frequency with the help of a resonator. But to produce a continuous frequency spectrum, the laser should be constructed in a way that to work in the chaotic regime.

6. *Celestial mechanics.* The Hénon-Heiles model (2.2) belongs to this field of science. The stochastic mechanics explains, in particular, why it is necessary to correct the trajectory of motion of a satellite or rocket from time to time.

7. *Chemistry, biology etc.* As the last example we note that the logistic map (2.9) has been introduced by P.F. Verhulst as far as in 1845 to simulate the evolution of a population in a closed area. Namely, if we denote by x_n the relative (normalized) number of species in the n-th year, the linear on x term in the

right-hand side of Eq. (2.9) will describe an increasing of the population due to duplication of species, while the quadratic term, their ruin owing to limits of meal resources, territory, *etc.*